Supporting Information

Boosting Power Output of the Cement-based Triboelectric Nanogenerator by Enhancing Dielectric Polarization with Highly Dispersed Carbon Black Nanoparticles Toward Large-scale Energy Harvesting from Human Footsteps

Saman Kuntharin[†], Viyada Harnchana[†,‡], Annop Klamchuen[§], Kitiphat Sinthiptharakoon[§], Prasit Thongbai[†,‡], Vittaya Amornkitbamrung[†,‡], Prinya Chindaprasirt[||]*

†Department of Physics, Khon Kaen University, Khon Kaen 40002, Thailand

[‡]Institute of Nanomaterials Research and Innovation for Energy (IN-RIE), Khon Kaen University, Khon Kaen, 40002, Thailand

[§]National Nanotechnology Center (NANOTEC), NSTDA, 111 Thailand Science Park, Paholyothin Road, Klong Luang, Pathum Thani 12120, Thailand

[||]Sustainable Infrastructure Research and Development Center, Department of Civil Engineering, Faculty of Engineering, Khon Kaen University, Khon Kaen 40002, Thailand; and The Academy of Science, Royal Society of Thailand, Dusit, Bangkok, 10300, Thailand

**Email:* viyada@kku.ac.th

Number of pages: 9

Number of figures: 5

Number of tables: 3

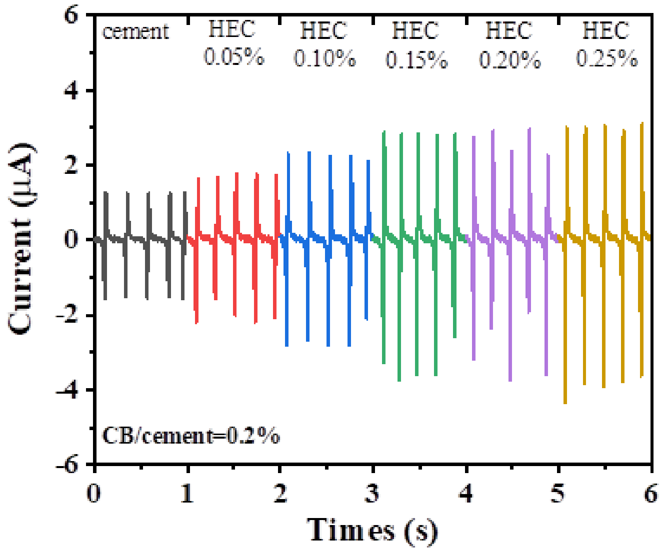

Figure S1 Output current of cement-CB@HEC at HEC concentration of 0.05-0.25%wt and CB concentration was controlled at 0.20%wt.

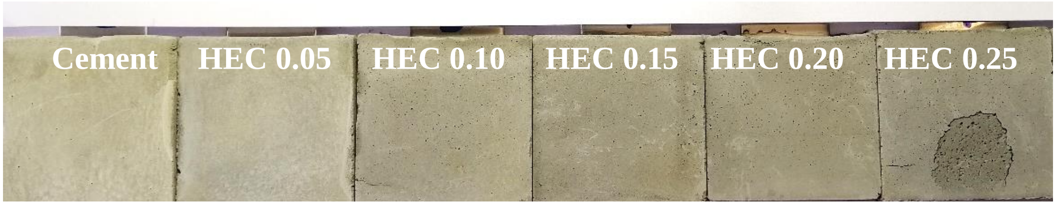

Figure S2 Digital photograph of hardened cement and cement-CB@HEC at HEC concentration of 0.05-0.25%wt

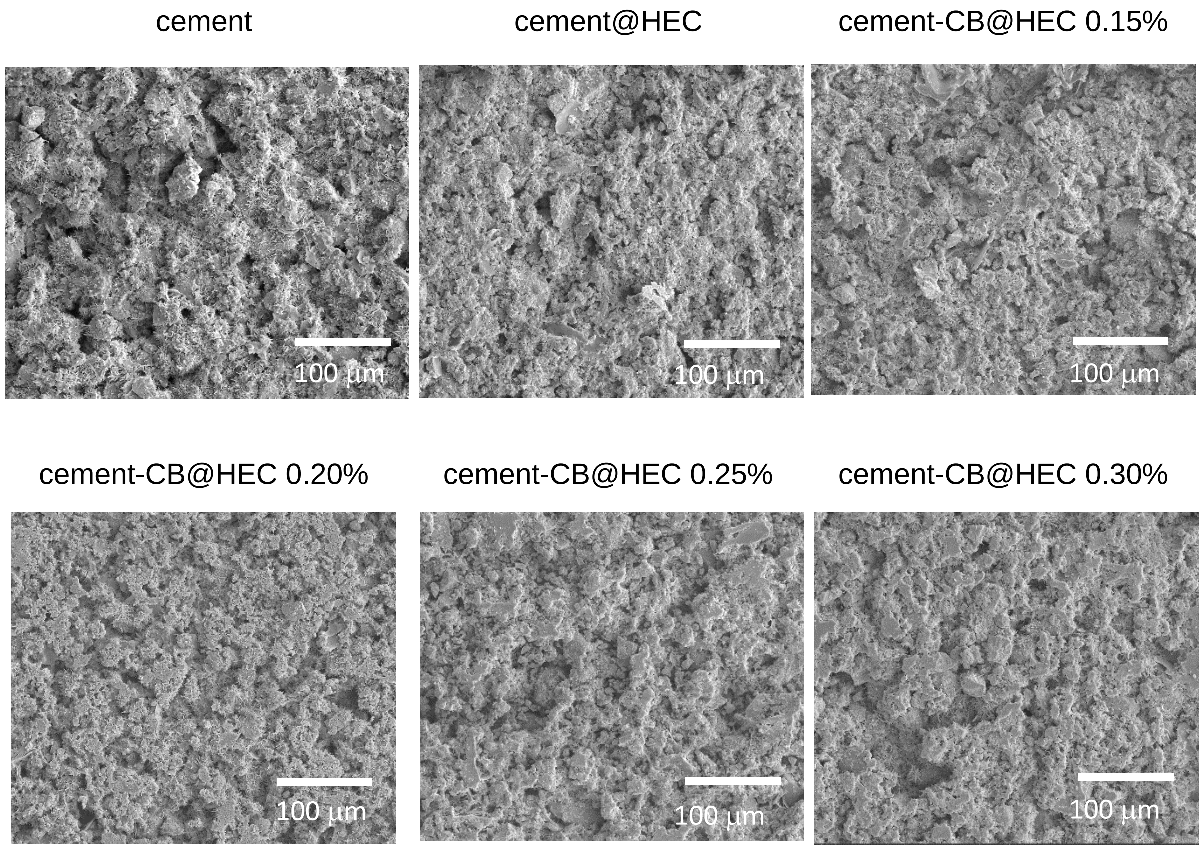

Figure S3 SEM images presenting surface morphologies of pristine cement and cement-CB@HEC 0-0.30%.

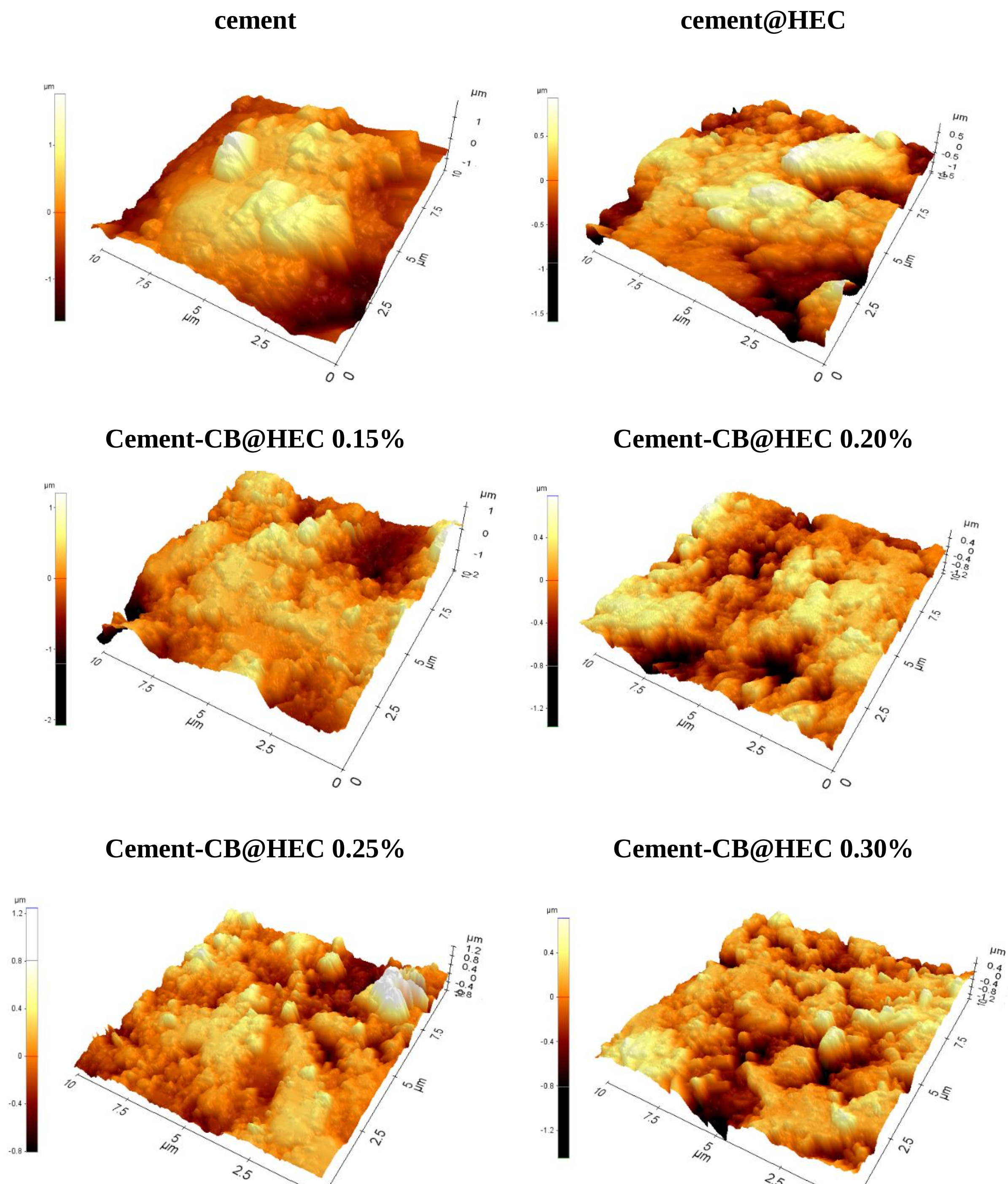

Figure S4 AFM surface topography maps of pristine cement and cement-CB@HEC 0-0.30%.

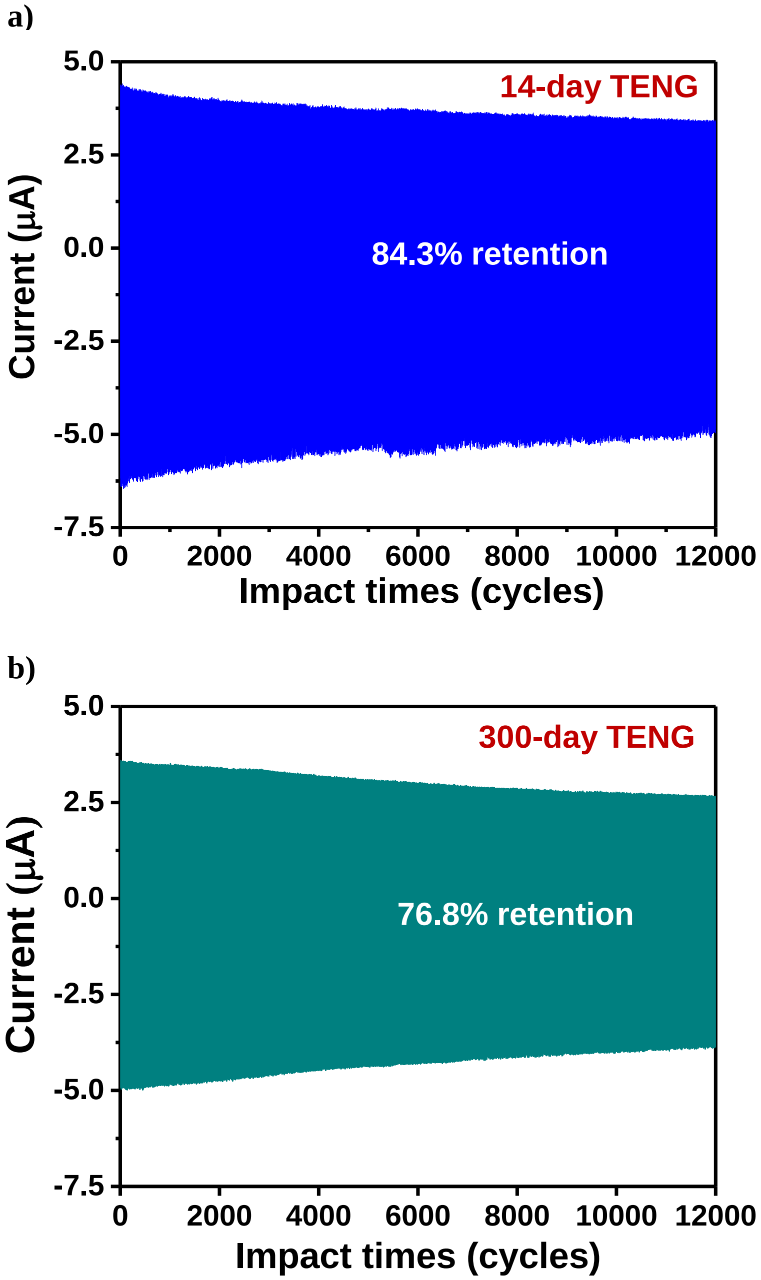

Figure S5 TENG performance stability of a) the 14-day and b) 300-day cement-CB@HEC 0.25% TENGs tested over 12,000 cycles

Table S1 Dielectric properties including constant (ε_r) and dielectric loss (tan δ), and electrical outputs of cement and cement-CB@HEC 0-0.30% composites.

Specimen	Fabrication detail: Filler fraction %wt		**Dielectric properties at 1 kHz**		**Electrical output**	
	HEC	CB	**ε_r**	**tan δ**	**V_{pp}(v)**	**I_{pp}(μA)**
cement	-	-	29.3	0.53	32	2.8
cement-CB@0.05%HEC	**0.05**	0.20	-	-	45	4.0
cement-CB@0.10%HEC	**0.10**	0.20	-	-	56	5.2
cement-CB@0.15%HEC	**0.15**	0.20	-	-	70	6.6
cement-CB@0.20%HEC	**0.20**	0.20	-	-	74	6.8
cement-CB@0.25%HEC	**0.25**	0.20	-	-	79	7.2
cement@HEC (no CB)	0.225	-	38.0	0.63	39	3.3
cement-CB@HEC 0.15%	0.225	**0.15**	44.7	0.46	67	6.0
cement-CB@HEC 0.20%	0.225	**0.20**	65.8	1.11	74	6.9
cement-CB@HEC 0.25%	0.225	**0.25**	101.0	0.87	109	9.1
cement-CB@HEC 0.30%	0.225	**0.30**	88.5	1.01	94	8.8

Table S2 The calculated RMS roughness and surface area values from AFM topography maps of cement and cement-CB@HEC 0-0.30%.

Specimen	RMS roughness (μm)	Surface area $(\mu m)^2$
cement	0.540	139
Cement@HEC	0.385	151
cement-CB@HEC 0.15%	0.378	163
cement-CB@HEC 0.20%	0.283	159
cement-CB@HEC 0.25%	0.252	167
cement-CB@HEC 0.30%	0.259	172

Table S3 Matched load resistances, the output voltage and current at matched load, and power density of the cement-CB TENG compared to some of preciously reported TENGs.

TENG	**Matched load (MΩ)**	**Output voltage at matched load**	**Output current at matched load (μA)**	**Power density (W/m^2)**	**reference**
cement-CB	0.8	55	69	2.38	This work
cement-TiO_2	5	46	9.2	0.265	[1]
cement-based conductive	40	13	0.8	0.051	[2]
metal–organic framework (MOF) of the zeolitic imidazole	20	3.5	3.5	0.392	[3]
Ferroelectric multilayer nanocomposite TENG	100	40	0.7	0.294	[4]
$(Ba_{0.838}Ca_{0.162})(Ti_{0.9072}Zr_{0.092})O_3$ (BCZTO)/ PDMS and $Ba(Ti_{0.8}Zr_{0.2})O_3$ (BZTO)/PDMS hybrid Piezo-TENG	100	300	12	3.5	[5]

References

(1) Sintusiri, J.; Harnchana, V.; Amornkitbamrung, V.; Wongsa, A.; Chindaprasirt, P. Portland Cement-TiO2 triboelectric nanogenerator for robust large-scale mechanical energy harvesting and instantaneous motion sensor applications. *Nano Energy* **2020**, *74*, 104802. DOI: 10.1016/j.nanoen.2020.104802.
(2) Ra, Y.; You, I.; Kim, M.; Jang, S.; Cho, S.; Kam, D.; Lee, S.-J.; Choi, D. Toward smart net zero energy structures: Development of cement-based structural energy material for contact electrification driven energy harvesting and storage. *Nano Energy* **2021**, *89*, 106389. DOI: https://doi.org/10.1016/j.nanoen.2021.106389.
(3) Khandelwal, G.; Chandrasekhar, A.; Maria Joseph Raj, N. P.; Kim, S. J. Metal–Organic Framework: A Novel Material for Triboelectric Nanogenerator–Based Self-Powered Sensors and Systems. *Advanced Energy Materials* **2019**, *9* (14), 1803581. DOI: 10.1002/aenm.201803581.
(4) Park, Y.; Shin, Y.-E.; Park, J.; Lee, Y.; Kim, M. P.; Kim, Y.-R.; Na, S.; Ghosh, S. K.; Ko, H. Ferroelectric Multilayer Nanocomposites with Polarization and Stress Concentration Structures for Enhanced Triboelectric Performances. *ACS Nano* **2020**, *14* (6), 7101-7110. DOI: 10.1021/acsnano.0c01865.
(5) Wang, W.; Zhang, J.; Zhang, Y.; Chen, F.; Wang, H.; Wu, M.; Li, H.; Zhu, Q.; Zheng, H.; Zhang, R. Remarkably enhanced hybrid piezo/triboelectric nanogenerator via rational modulation of piezoelectric and dielectric properties for self-powered electronics. *Applied Physics Letters* **2020**, *116* (2), 023901. DOI: 10.1063/1.5134100.